Biophysical Journal
Article

Biophysical Society

Spatial Cytoskeleton Organization Supports Targeted Intracellular Transport

Anne E. Hafner[1] and Heiko Rieger[1,*]
[1]Department of Theoretical Physics and Center for Biophysics, Saarland University, Saarbrücken, Germany

ABSTRACT The efficiency of intracellular cargo transport from specific sources to target locations is strongly dependent upon molecular motor-assisted motion along the cytoskeleton. Radial transport along microtubules and lateral transport along the filaments of the actin cortex underneath the cell membrane are characteristic for cells with a centrosome. The interplay between the specific cytoskeleton organization and the motor performance results in a spatially inhomogeneous intermittent search strategy. To analyze the efficiency of such intracellular search strategies, we formulate a random velocity model with intermittent arrest states. We evaluate efficiency in terms of mean first passage times for three different, frequently encountered intracellular transport tasks: 1) the narrow escape problem, which emerges during cargo transport to a synapse or other specific region of the cell membrane; 2) the reaction problem, which considers the binding time of two particles within the cell; and 3) the reaction-escape problem, which arises when cargo must be released at a synapse only after pairing with another particle. Our results indicate that cells are able to realize efficient search strategies for various intracellular transport tasks economically through a spatial cytoskeleton organization that involves only a narrow actin cortex rather than a cell body filled with randomly oriented actin filaments.

INTRODUCTION

Intracellular transport of various cargoes from specific origins to target locations is crucial for the correct function of cells and organisms. The cytoskeleton is a self-organizing filamentous network that shapes the mechanical and rheological characteristics of the cell (1–5), drives cell motility or division (6), and coordinates cargo transport between different cellular regions (7–9). The main components of the cytoskeleton that are involved in intracellular transport are the polarized microtubules and actin filaments. Associated motor proteins walk actively along these filaments as they simultaneously bind to cargo particles (10,11). Kinesin and dynein motors, which run on microtubules, cooperate in transport with myosin motors, which walk on actin filaments. Several motors of diverse species are attached to one cargo concurrently (12–16). Correct cargo delivery thus depends on the coordination of microtubule- and actin-based transport. Experimental data suggest that such coordination is achieved by regulation of the respective motor species activity through signaling processes (16–19). A prominent example is the transfer of pigment granules between the actin and the microtubule network of melanophores, which is tightly controlled by the intracellular level of cyclic adenosine monophosphate (20).

Furthermore, intracellular transport switches between two modes of motility; ballistic motion along the cytoskeleton is interrupted by effectively stationary states (21). Cargo-motor complexes frequently pause because of mechanical constraints by intersection nodes of the cytoskeleton and potentially cycles of detachment and reattachment processes in the crowded cytoplasm, which subsequently lead to a reorientation of the transport direction (12,22–26). The run-and-pause behavior of cargo influences the diffusional properties (27) as well as the efficiency of intracellular transport.

Typically, cargo, like proteins, vesicles, and other organelles, emerges in one region of the cell but is needed in some other area or has to fuse with a mobile reaction partner. In the absence of a direct connection between searcher and target, the transport is a stochastic process with random alternation between ballistic motion and reorienting arrest states, which is denoted as intermittent search (28). A particular set of parameters defining this stochastic process, such as the switching rates between ballistic transport and pauses, represents a specific intermittent search strategy.

Submitted September 15, 2017, and accepted for publication January 30, 2018.

*Correspondence: h.rieger@mx.uni-saarland.de

Editor: Sean Sun.
https://doi.org/10.1016/j.bpj.2018.01.042

The efficiency of a search strategy is commonly evaluated in terms of the mean first passage time that a randomly moving particle needs to find a target. It has been shown that tuning the search parameters can substantially decrease the mean first passage time in homogeneous and isotropic environments, i.e., under the assumption of a spatially constant density of filament orientations with no preferred direction. For instance, it has been determined that an optimal choice of the switching rates enhances the efficiency of intermittent search strategies (28–31), and the search of small targets on the surface of spherical domains also benefits from modulated phases of surface-mediated and bulk diffusion (32,33). Moreover, it has recently been shown that intracellular transport can profit from inhomogeneous cytoskeletal organizations by demonstrating that the transit time from the nucleus to the whole cell boundary can be reduced by confining the cytoskeleton to a delimited shell within the cell (34).

However, real cell cytoskeletons display a complex spatial organization that is neither homogeneous nor isotropic. For instance, in cells with a centrosome, the microtubules emanate radially from the central microtubule organizing center (MTOC) and actin filaments form a thin cortex underneath the plasma membrane, with a broad distribution of directions again centered around the radial direction (6) (see Fig. 1 *a* for a sketch). Consequently, the cytoskeleton is very inhomogeneous and characterized by a well-defined actin cortex (35,36). In essence, the specific spatial organization of the cytoskeleton represents, in conjunction with motor-assisted transport, an intermittent search strategy, which is probably optimized for specific frequently occurring transport tasks but less well-suited for others. It is still obscure how much the efficiency of diverse transport tasks is affected by the interplay between spatially inhomogeneous cytoskeleton organization, motor performance, and detection mode, in particular in comparison to homogeneous search strategies.

Here, we investigate this question by formulating a random velocity model with intermittent arrest states in spatially inhomogeneous environments. With the aid of computer simulations, we analyze the search in terms of the mean first passage time to detection for three basic tasks, which are frequently encountered in intracellular transport:

1) Transport of cargo from an arbitrary position within the cell, typically from a location close to the nucleus, to a specific area on the plasma membrane. For instance, directed secretion by immune cells requires the formation of an immunological synapse (37,38), and transport of secretion material toward the synapse involves active motion along the cytoskeleton (39,40). Active transport toward a specific area on the plasma membrane is also required to reinforce spatial asymmetries of proteins that regulate polarized cell functions (such as Cdc42 in budding yeast (41)), to induce the outgrowth of dendrites or axons from neurons (42,43), or to recover plasma membrane damages (44,45). The stochastic search for a specific small area on the boundary of a search domain is reminiscent of the so-called narrow escape problem (46,47). Here we ask whether the specific organization of the cytoskeleton, as sketched in Fig. 1 *a*, has the potential to solve the narrow escape problem more efficiently than the homogeneous pendant.
2) The enhancement of the reaction kinetics between two reaction partners by motor-assisted transport. We consider the binding time of two independently moving particles within the cell such as fusing vesicles, e.g., late

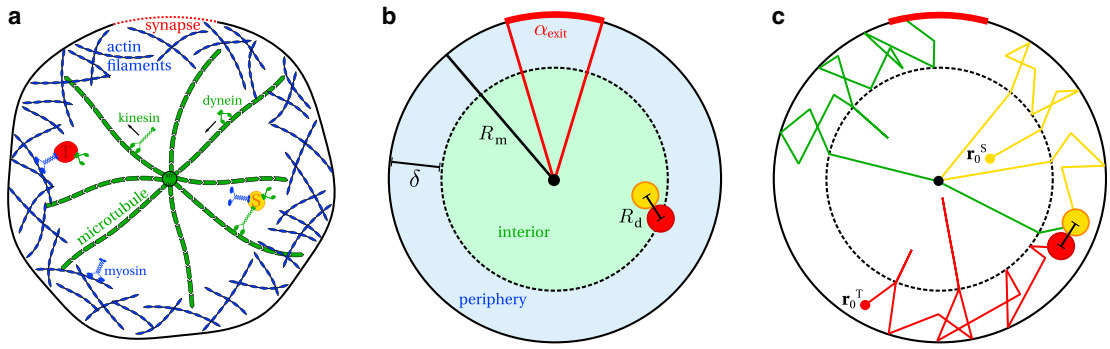

FIGURE 1 Random velocity model for intracellular search processes. (*a*) Targeted intracellular transport by kinesin, dynein, and myosin motor proteins is a stochastic process that strongly depends on the spatial organization of the cytoskeleton. The cytoskeleton of cells with a centrosome is generally inhomogeneous. Although microtubules emanate radially from the central MTOC, actin filaments accumulate in the cortical layer underneath the plasma membrane and exhibit random orientations. (*b*) We idealize the cytoskeleton structure in a spherical cell of radius R_{m} by introducing a well-defined actin cortex of width δ that splits the cytoplasm into interior and periphery. An exit zone on the cell boundary is characterized by the angle α_{exit}, and the detection distance of two particles is determined by R_{d}. (*c*) In the combined reaction-escape problem, two mobile particles which are initially located at $\boldsymbol{r}_0^S$, $\boldsymbol{r}_0^T$ perform a stochastic motion until they detect each other. After the reaction, the product particle is stochastically transported to the exit zone on the plasma membrane, as sketched by the green trajectory, where the reaction-escape problem is terminated. To see this figure in color, go online.

endosomes and lysosomes (6,48). In particular, we check for the impact of an inhomogeneous cytoskeleton organization and two different reaction modes. In the context of intermittent search strategies, it is typically assumed that detection is only possible in the phase of slow displacement (28,49,50), i.e., in the waiting state. Although some experimental data suggest a connection between mobility of particles and likelihood of reactions (51,52), it remains elusive whether this assumption is valid for all chemical reactions that take place inside living cells. Therefore, we study two possible detection modes. Reaction may either be possible by simple encounter, no matter what state both particles possess, or it may exclusively be possible when both particles are in the waiting state.

3) Finally, the combination of the reaction and escape problem, in which cargo first has to bind to a reaction partner before it can be delivered or dock at a specific area of the cell boundary such as a synapse. A prominent realization is the docking of lytic granules at the immunological synapse of cytotoxic T-lymphocytes (37,39,40), which requires them to pair with CD3-containing endosomes beforehand (53). Lytic granules have a low docking probability at the synapse, whereas endosomes loaded with CD3 receptors have a high docking probability. Apparently, it represents an advantageous strategy to tether lytic granules and CD3 endosomes first to guarantee the delivery of cytotoxic cargo exclusively to the synapse. We analyze how the spatial organization of the cytoskeleton supports the efficiency of this strategy for different reaction modes.

In the following, we refer to these three problems of intracellular transport as 1) the narrow escape problem, 2) the reaction problem, and 3) the reaction-escape problem.

Our goal is to show that in all cases, spatially inhomogeneous intermittent search strategies exist that are more efficient than their homogeneous counterpart and that are actually realized by the spatial organization of the cytoskeleton of cells with a centrosome (see Fig. 1 *a*).

In the following, we present an extension of (54). There we focused on the narrow escape problem for random walks with intermittent arrest states. Here we study in addition the reaction and the reaction-escape problem in inhomogeneous environments. Our results are in agreement with recent findings for inhomogeneous search strategies with intermittent diffusion in the limit of a vanishing diffusion coefficient (49,50). In contrast to (49,50), we systematically study the impact of pausing states on the efficiency of intracellular transport task. We further explore the impact of the detection mode on the reaction kinetics, focus on mobile reaction partners with identical as well as nonidentical motility properties, and take several steps toward a more realistic distribution of cytoskeleton filaments.

METHODS

For this purpose, we present a coarse-grained perspective on intracellular transport by exploring the effective cargo movement and neglecting the stepping of individual motors at the molecular level. We formulate an intermittent random velocity model in continuous two-dimensional (2D) space and time in which a particle performs a random walk with two alternating motility modes: 1) a ballistic motion state at velocity $\boldsymbol{v}(v,\phi_v)$, which is associated to directed transport by molecular motors between binding and unbinding events, and 2) a waiting state, in which motors are unbound or particles are stuck at filament crossings. The speed v is assumed to be constant throughout the following. Transitions from motion to waiting state (waiting to motion state) are determined by a constant rate $k_{m\to w}$ ($k_{w\to m}$). Hence, the residence times t_m and t_w in each state of motility are exponentially distributed as follows:

$$p(t_m) = k_{m\to w} e^{-k_{m\to w} t_m} \tag{1}$$

and

$$p(t_w) = k_{w\to m} e^{-k_{w\to m} t_w}, \tag{2}$$

with mean values $1/k_{m\to w}$ and $1/k_{w\to m}$. This is biologically reasonable, as active lifetimes of cargoes are reported to be exponentially distributed (55). Whereas the rate $k_{m\to w}$ represents the detachment rate of the particle, $k_{w\to m}$ defines the mean waiting time per arrest state.

After a waiting period, the particle changes its direction of motion according to a characteristic rotation angle $\alpha_{\rm rot}$ that reflects the specific spatial organization of the cytoskeleton. We idealize the cytoskeleton of a spherical cell with radius $R_{\rm m}$ by introducing a well-defined actin cortex of width δ underneath the plasma membrane, which splits the cytoplasm into interior and periphery, as sketched in Fig. 1 *b*. Although the interior only contains microtubules, which emanate radially from the central MTOC, the periphery is dominated by randomly oriented actin filaments. With regard to the spatial organization of the cytoskeleton, the walking direction $\phi_v = \phi_r + \alpha_{\rm rot}$ is updated with respect to the polar angle of the current position $\boldsymbol{r}(r,\phi_r)$ and the rotation angle $\alpha_{\rm rot}$ is drawn from the idealized distribution,

$$f(\alpha_{\rm rot}) = \begin{cases} p_{\rm antero}\,\delta(\alpha_{\rm rot}) + (1-p_{\rm antero})\delta(\alpha_{\rm rot}-\pi), & \text{for } 0<r<R_{\rm m}-\delta, \\ 1/(2\pi), & \text{for } R_{\rm m}-\delta<r<R_{\rm m}, \end{cases} \tag{3}$$

where $p_{\rm antero}$ is the probability for anterograde transport (radially outward transport along microtubule plus direction) and $(1-p_{\rm antero})$ is the probability for retrograde transport (radially inward transport along microtubule minus direction). Hence $p_{\rm antero}$ reflects the activity level of a particular motor species. For instance, $p_{\rm antero}=0$ corresponds to a high activity of dyneins, which carry the cargo to the cell center, whereas for $p_{\rm antero}=1$, the cargo is mainly transported in the periphery by myosins. Intermediate values of $p_{\rm antero}$ enable a frequent exchange between microtubule- and actin-based

transport. The distribution of velocity directions given by Eq. 3 depends on the current particle position $\boldsymbol{r}$ within the cell, which accounts for the inhomogeneity of the cytoskeleton. The distribution $f(\alpha_{\mathrm{rot}})$, together with the state transition rates $k_{m\to w}$ and $k_{w\to m}$, defines a search strategy which is generally inhomogeneous and anisotropic. Here, the special case $\delta = R_{\mathrm{m}}$ leads to a spatially homogeneous and isotropic search strategy.

At time $t = 0$, we assume the particle to start its search in the motion state at position $\boldsymbol{r}_0$, which may either be uniformly distributed throughout the cell ($f(r_0) = 1/R_{\mathrm{m}}, f(\phi_{r_0}) = 1/(2\pi)$) or deterministically at the center of the cell ($r = 0$). Apart from stochastic transitions to the waiting state with rate $k_{m\to w}$, a ballistically moving particle pauses automatically at the MTOC ($r = 0$), at the inner border of the actin cortex ($r = R_{\mathrm{m}} - \delta$), and at the cell membrane ($r = R_{\mathrm{m}}$), where the rotation angle distribution $f(\alpha_{\mathrm{rot}})$ is restricted to available values. For the narrow escape problem, the search is terminated when the particle hits the plasma membrane at the exit zone of opening angle α_{exit}, as illustrated in Fig. 1 *b*. In the case of the reaction problem, the search is terminated by encounter of searcher and target particle ($\left|\boldsymbol{r}^{\mathrm{S}} - \boldsymbol{r}^{\mathrm{T}}\right| = R_{\mathrm{d}}$, see Fig. 1, *b* and *c*) either regardless of their motility state or only possible in the waiting state. Reaction takes place instantaneously. In the reaction-escape problem, searcher and target particle first have to react before the newly formed product particle can be transported to a specific zone on the membrane of the cell. In the following, we use rescaled, dimensionless spatial and temporal coordinates $\boldsymbol{r}\mapsto\boldsymbol{r}/R_{\mathrm{m}}$ and $t\mapsto vt/R_{\mathrm{m}}$ and parameters $k_{m\to w}\mapsto R_{\mathrm{m}}k_{m\to w}/v$, $k_{w\to m}\mapsto R_{\mathrm{m}}k_{w\to m}/v$, and $\delta\mapsto\delta/R_{\mathrm{m}}$.

The efficiency of a search strategy, defined by a specific cytoskeleton organization and motor performance, is measured in terms of a mean first passage time (MFPT) with respect to the events defined by the different search problems. To calculate the MFPT, we use an event-driven Monte Carlo algorithm to generate the stochastic process, as sketched in Fig. 1 *c*, and calculate the MFPT as an ensemble average. We use roughly 10^6 independent realizations of the search process for each parameter value such that the relative statistical error for the MFPT is significantly lower than 0.5%.

RESULTS

The proposed model allows the study of diverse transport tasks. Here we focus on three different, biologically relevant search problems: the narrow escape, the reaction, and the reaction-escape problem. We analyze the dependence of the search efficiency on the spatial organization of the cytoskeleton as well as the detection mode and the motor performance.

Narrow escape problem

First, we consider intracellular transport of cargo that is initially either centered or uniformly distributed within the cell to a specific area on the plasma membrane. We evaluate the impact of a particular spatial organization of the cytoskeleton given by Eq. 3 on the search efficiency.

To demonstrate the gain in efficiency of a spatially inhomogeneous search strategy corresponding to $0 < \delta < 1$, we first consider homogeneous cytoskeleton organizations with $\delta = 1$. In accordance with (54), we find that the MFPT decreases monotonically with increasing target size α_{exit} for diverse values of the transition rates $k_{m\to w}$ and $k_{w\to m}$, as shown in Fig. 2, *a* and *b*. Fig. 2, *a* and *b* further displays that initially uniformly distributed searcher positions are slightly more advantageous than a deterministic initial position at the cell center for large target sizes. For large exit zones $\alpha_{\mathrm{exit}} \approx 2\pi$, the searcher is likely to find the escape by first encounter with the membrane; hence the initial location of the searcher has a strong influence on the MFPT. Contrarily, for narrow escapes, many hitting events with the membrane are necessary to find the exit zone, and as a result, the impact of the initial position of the searcher vanishes, as the findings in Fig. 2, *a* and *b* demonstrate. Moreover, Fig. 2, *a* and *b* indicates that an increase in the rate $k_{m\to w}$ as well as a decrease in $k_{w\to m}$ hinders the detection of targets alongside the membrane. Accordingly, Fig. 2 *c* illustrates that the optimal choice of the transition rates for a search on a homogeneous cytoskeleton is given by $k^{\mathrm{opt}}_{m\to w} = 0$ and $k^{\mathrm{opt}}_{w\to m} = \infty$. Consequently, an uninterrupted motion pattern without directional changes in the bulk of the cell constitutes an optimal search strategy for a homogeneous cytoskeleton ($\delta = 1$). In the following, we ask whether an inhomogeneous filament structure ($\delta < 1$) has the potential to solve the narrow escape problem more efficiently than its homogeneous pendant.

To answer this question, we compute the influence of the actin cortex width δ on the MFPT for various parameters $k_{m\to w}$, $k_{w\to m}$, and p_{antero} for small escape regions of angle $\alpha_{\mathrm{exit}} = 0.1$. Note that in this case, the exit zone constitutes only 1.59% of the total spherical surface. Remarkably, we find that for large probabilities of anterograde transport p_{antero}, the MFPT exhibits a pronounced minimum at small widths of the actin cortex δ. This phenomenon is largely robust against changes in the transition rates $k_{m\to w}$ and $k_{w\to m}$. The MFPT can be split into the total mean motion time (MMT) and the total mean waiting time (MWT) a particle experiences in the course of its search. Thereby, the mean waiting time is the product of the total mean number of waiting periods (# waiting periods) and the mean waiting time per arrest state ($1/k_{w\to m}$). In (54), we showed that the number of waiting periods is independent of $k_{w\to m}$ and defines the optimal width of the actin cortex δ in the limit of $k_{w\to m}\to 0$. Consistent with (54), Fig. 2, *d* and *e* demonstrate that the MMT, which defines the MFPT for $k_{w\to m}\to\infty$, as well as the mean number of waiting periods, display prominent minima as a function of δ for large probabilities p_{antero} for anterograde transport. Note that the first passage time distribution, which for Brownian motion in bounded domains generally consists of three parts (short times: exponential decay, intermediate times: power law, long times: exponential decay) (56,57), exhibits a broadening of the intermediate power law regime for $\delta\to 0$, as shown in the inset of Fig. 2 *e*. However, when the search is dominated by radially inward transport for small p_{antero}, a homogeneous strategy $\delta = 1$ is most efficient, since $\delta \neq 1$ and $p_{\mathrm{antero}} = 0$ prevents the searcher from touching the membrane. Nonetheless, Fig. 2 *f* shows that a small cortex width δ potentially reduces the MFPT by several orders of magnitude. This emphasizes the general enhancement of the search efficiency

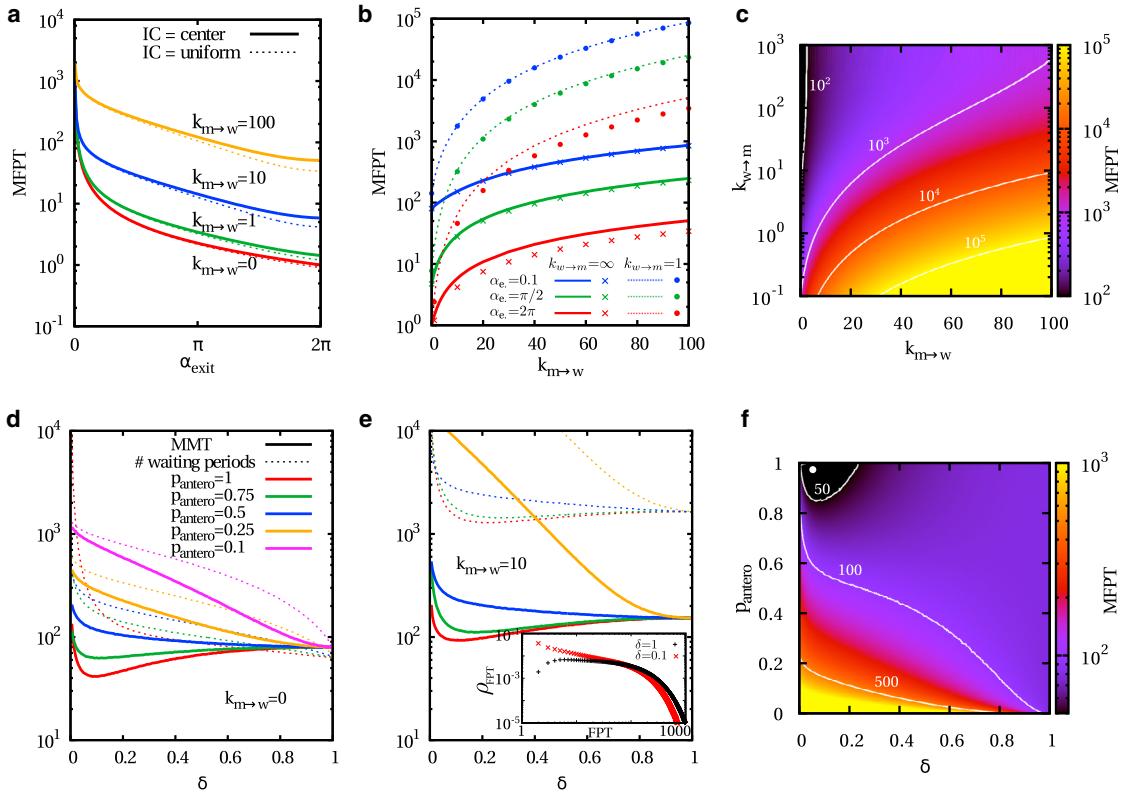

FIGURE 2 Narrow escape problem for homogeneous and inhomogeneous spatial organizations of the cytoskeleton. (*a*) Shown here is the MFPT versus the target size α_{exit} for different values of the transition rate $k_{m\to w}$ and $k_{w\to m} = \infty$ on a homogeneous cytoskeleton structure. Dashed lines correspond to initially uniformly distributed searcher positions, and solid lines refer to searchers that are initially located at the center of the cell. (*b*) Shown here is the MFPT versus $k_{m\to w}$ for a homogeneous cytoskeleton organization and diverse target sizes α_{exit} and rates $k_{w\to m}$. Lines correspond to the centered initial condition, and symbols correspond to the uniform case. (*c*) Shown here is the MFPT for a homogeneous cytoskeleton organization and centered initial condition as a function of the transition rates $k_{m\to w}$ and $k_{w\to m}$ for $\alpha_{\text{exit}} = 0.1$. (*d*) Shown here are the MMT and the mean number of waiting periods against the width of the actin cortex δ, which defines the inhomogeneity of the cytoskeleton, for diverse p_{antero}, $k_{m\to w} = 0$, centered initial condition, and exit size $\alpha_{\text{exit}} = 0.1$. (*e*) Shown here is the same as in (*d*), but for $k_{m\to w} = 10$. The inset shows the full distribution of first passage times for $k_{m\to w} = 10$, $k_{w\to m} = \infty$, $p_{\text{antero}} = 1$, and centered initial condition with $\delta = 1$ and $\delta = 0.1$. At intermediate timescales, a broadening of the power law regime is observed for $\delta \to 0$. (*f*) Shown here is the MFPT versus δ and p_{antero} for $k^{\text{opt}}_{m\to w} = 0$ and $k^{\text{opt}}_{w\to m} = \infty$, which constitutes the optimal choice of transition rates for a spatially homogeneous cytoskeleton, and centered initial condition of the searcher in the case of $\alpha_{\text{exit}} = 0.1$. To see this figure in color, go online.

by a spatially inhomogeneous filament structure compared to the homogeneous pendant.

Reaction problem

Next, we investigate how efficient a spatial organization of the cytoskeleton as defined in Eq. 3 can actually be for the reaction problem. Two mobile particles with identical properties and uniformly distributed initial positions perform random motion inside the cell until they detect each other and react. We consider two different reaction modes that depend on the motility states of both particles. On the one hand, searcher and target particle react by simple encounter $\left|\boldsymbol{r}^{\text{S}} - \boldsymbol{r}^{\text{T}}\right| = R_{\text{d}}$ regardless of the state both are in. On the other hand, detection is only possible when searcher and target particle are in the waiting state and their relative distance is smaller than the detection radius $\left|\boldsymbol{r}^{\text{S}} - \boldsymbol{r}^{\text{T}}\right| \leq R_{\text{d}}$. Fig. 1 *c* includes a sketch of the reaction problem.

Fig. 3, *a–d* show the results for the MFPT in the case of a spatially homogeneous cytoskeleton ($\delta = 1$) as a function of the transition rates $k_{m\to w}$ and $k_{w\to m}$ for two different detection radii, $R_{\text{d}} = 0.1$ and $R_{\text{d}} = 0.025$. Although Fig. 3, *a* and *b* show that the optimal choice of transition rates is $k^{\text{opt}}_{m\to w} = 0$ and $k^{\text{opt}}_{w\to m} = \infty$ for detection by simple encounter, a nontrivial optimum arises when reaction is only possible in the waiting state, as shown in Fig. 3, *c* and *d*. Remarkably, the absolute values of the minima are rather robust against alterations of the transition rates, as indicated by the contour lines. Moreover, Fig. 3 *e* illustrates that for high values of $k_{m\to w}$, the MFPT is largely independent of the detection mode. The detection time is then dominated by getting the particles in close proximity in the first place.

We take the optimal values $k^{\text{opt}}_{m\to w}$ and $k^{\text{opt}}_{w\to m}$ from the homogeneous case $\delta = 1$ and compute the MFPT for an inhomogeneous cytoskeleton organization as a function of the actin cortex width δ and the probability for radially outward transport p_{antero}. The results, shown in Fig. 4, *a* and *b*,

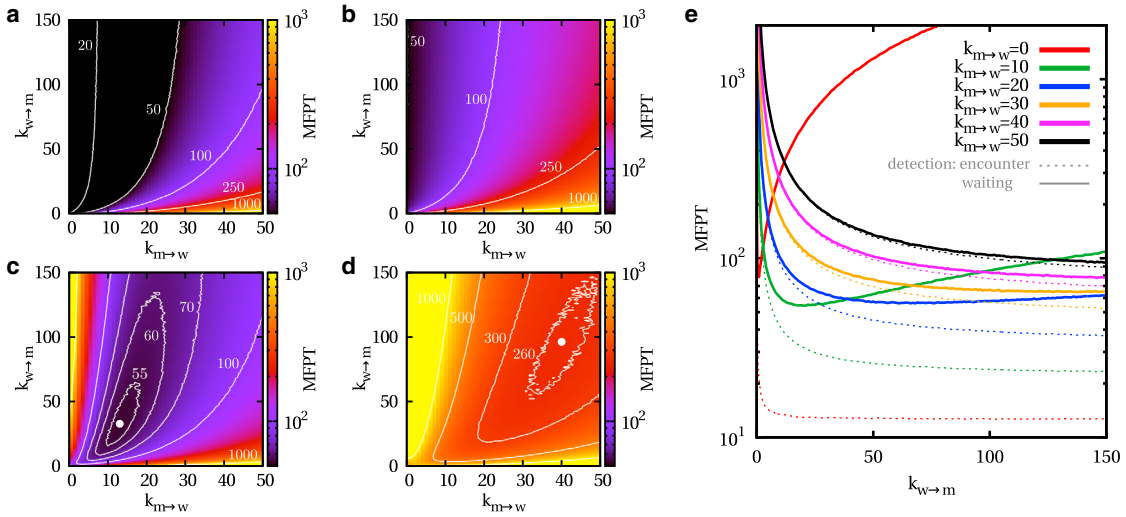

FIGURE 3 Reaction problem for homogeneous organizations of the cytoskeleton. (*a*) Shown here is the MFPT versus $k_{m\to w}$ and $k_{w\to m}$ for $R_d = 0.1$ and detection by simple encounter. (*b*) Shown here is the same as in (*a*), but for $R_d = 0.025$. (*c*) Shown here is the MFPT versus $k_{m\to w}$ and $k_{w\to m}$ for $R_d = 0.1$ and detection that is only possible in the waiting state. (*d*) Shown here is the same as in (*c*), but for $R_d = 0.025$. (*e*) Shown here is the MFPT in dependence of $k_{w\to m}$ for diverse rates $k_{m\to w}$, $R_d = 0.1$, and both detection modes. To see this figure in color, go online.

demonstrate that for both detection modes, a superior strategy can be found for $p_{antero} = 0$, which drives the particles toward the central MTOC. Fig. 4, *c–e* show that a cell is able to regulate the location of the reactions, and thus the spatial distribution of reaction products, by adjustment of p_{antero}. Although for $p_{antero} = 0$, reaction mainly takes place in the interior of the cell close to the central MTOC, it predominantly happens in the peripheral actin cortex for $p_{antero} = 1$. Note that the peaks in Fig. 4, *c* and *d* at radial positions $r = R_d$ and $r = R_m - R_d$ arise because of the detection radius, which is here set to $R_d = 0.1$. Furthermore, the peaks at $r \in \{0; \delta; R_m\}$ result from automatic switching to the arrest state, which is particularly beneficial when detection is only possible in the waiting state. Besides the reaction strategy of moving searcher and target particle toward the MTOC by $p_{antero} = 0$, which is generally optimal for $\delta = 0$ as indicated by Fig. 4 *f*, the reaction time can also be minimized for $p_{antero} = 1$ by establishing a thin actin cortex, as shown in Fig. 4, *g* and *h*. The occurrence of the minimum depends critically on both transition rates. Fig. 4 *i* shows that the MMT as well as the number of waiting periods depend on $k_{m\to w}$ and $k_{w\to m}$. This is in sharp contrast to our findings for the narrow escape problem and holds in particular when detection is only possible in the waiting state.

Note that, for instance, the MFPT in Fig. 4, *h* and *i* displays a prominent kink at $\delta = 0.1$ for $k_{m\to w} = 0$ for detection in the waiting state. Under these conditions, a particle does not switch to the waiting state in the bulk of the cell, and consequently detection critically depends upon automatic transitions to the waiting state at the MTOC ($r = 0$), the inner border of the actin cortex ($r = 1 - \delta$), and the plasma membrane ($r = 1$). When $\delta \leq R_d$, there are three different realizations of searcher and target locations which may lead to detection: both particles at the membrane, both particles at the inner border, or one particle at the membrane and one at the inner border. When $1 - R_d \leq \delta$, there are again three possible configurations for detection: both particles at the inner border, both at the MTOC, or one at the inner border and one at the MTOC. However, for $R_d < \delta < 1 - R_d$, the mixed configurations are not possible anymore, and reaction can only take place when both particles are either located closely enough at the membrane or at the MTOC. This results in the kink of the MFPT at $\delta = 0.1$, since $R_d = 0.1$ in Fig. 4.

Reaction problem for nonidentical particles

Until now, we studied the reaction problem for searcher and target particles with identical motility pattern, i.e., with equal transition rates $k_{m\to w}$ and $k_{w\to m}$ and equal probability for anterograde transport p_{antero}. Here, we investigate consequences of nonidentical motility schemes on the efficiency of intracellular reactions. This is relevant when searcher and target particle are not equal but, e.g., are equipped with different motor species or differ in size. Waiting times and effective mesh size of the cytoskeleton, which are associated with the transition rates $k_{m\to w}$ and $k_{w\to m}$, depend on the size of the transported cargo (12).

To study the impact of nonidentical particle properties, we fix the motility parameters ($k^S_{m\to w}$, $k^S_{w\to m}$, and p^S_{antero}) of the searching particle, but vary the ones ($k^T_{m\to w}$, $k^T_{w\to m}$, and p^T_{antero}) of the target. Fig. 5 *a* displays the MFPT as a function of the width δ of the actin cortex for nonidentical values of p_{antero}. Although $p^S_{antero} = 1$ is fixed for the searcher, p^T_{antero} is varied for the target particle. Apart from

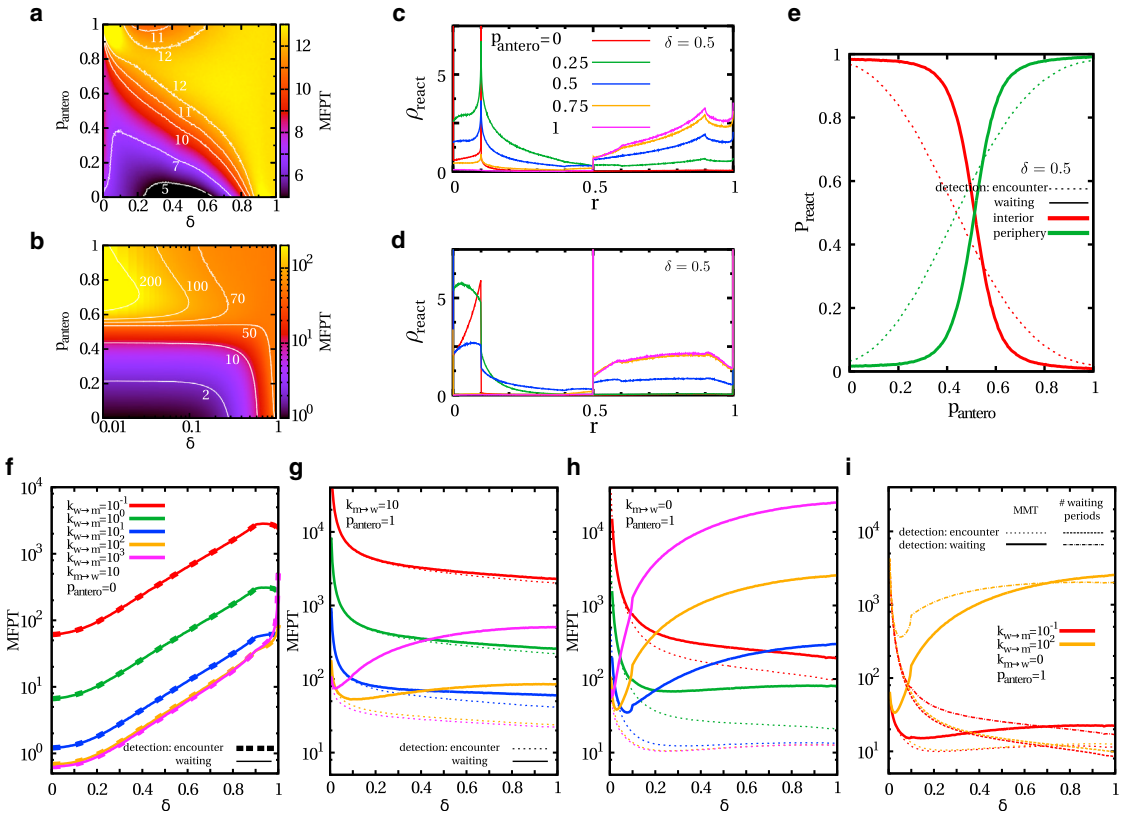

FIGURE 4 Reaction problem for inhomogeneous organizations of the cytoskeleton. (*a*) Shown here is the MFPT as a function of δ and p_{antero} for $R_{\text{d}} = 0.1$, $k^{\text{opt}}_{m\to w} = 0$, and $k^{\text{opt}}_{w\to m} = \infty$, which are the optimal rates for the homogeneous case when detection happens by simple encounter. (*b*) Shown here is the MFPT as a function of δ and p_{antero} for $R_{\text{d}} = 0.1$, $k^{\text{opt}}_{m\to w} = 13$, and $k^{\text{opt}}_{w\to m} = 34$, which are the optimal rates for the homogeneous case since detection is only possible in the waiting state. (*c*) Shown here is the distribution of reaction locations r for various values of p_{antero}. The cortical width is fixed to $\delta = 0.5$, and the transition rates $k^{\text{opt}}_{m\to w}$ and $k^{\text{opt}}_{w\to m}$ are applied. Detection takes place by encounter at $R_{\text{d}} = 0.1$. (*d*) Shown here is the same as in (*c*), but detection is only possible in the waiting state. (*e*) Given here is the probability for a reaction to take place in the interior or the periphery of a cell versus p_{antero} for fixed width of the actin cortex $\delta = 0.5$ and $R_{\text{d}} = 0.1$. The rates $k^{\text{opt}}_{m\to w}$ and $k^{\text{opt}}_{w\to m}$ are applied for both reaction modes. (*f*) Shown here is the MFPT as a function of the width of the actin cortex δ for $R_{\text{d}} = 0.1$, $p_{\text{antero}} = 0$, $k_{m\to w} = 10$, diverse values of $k_{w\to m}$, and both detection modes. (*g*) Shown here is the same as in (*f*), but for $p_{\text{antero}} = 1$. (*h*) Shown here is the same as in (*g*), but for $k_{m\to w} = 0$. (*i*) Shown here is the MMT as well as the mean number of waiting periods versus δ for $R_{\text{d}} = 0.1$, $p_{\text{antero}} = 1$, $k_{m\to w} = 0$, diverse values of $k_{w\to m}$, and both detection modes. To see this figure in color, go online.

that, the particles are identical. As expected, a strong inequality in p_{antero} increases the MFPT by several orders of magnitude as it drives the particles apart. Although the ones with $p_{\text{antero}} = 1$ are predominantly moving in the cortex, the ones with $p_{\text{antero}} = 0$ stick to the center of the cell. Consequently, a homogeneous search strategy on a random network with $\delta = 1$ is favorable in that case. This finding is robust against changes in the transition rates $k_{m\to w}$ and $k_{w\to m}$. Remarkably, the influence of nonidentical transition rates $k_{m\to w}$ and $k_{w\to m}$ on the search efficiency strongly depends on the detection mode, as found by Fig. 5, *b* and *c*. Although making the target less motile than the searcher, either by increasing $k^{\text{T}}_{m\to w}$ or decreasing $k^{\text{T}}_{w\to m}$, makes the search less efficient when detection takes place by pure encounter, it has the opposite effect when detection is only possible in the waiting state. This result is robust against changes in p_{antero} but vanishes for increasing $k_{m\to w}$, as the search is then first of all determined by getting the particles in close proximity.

Next, we analyze the consequences of an immotile target that is uniformly distributed in the cell on the efficiency of the reaction problem. Fig. 5 *d* shows the MFPT to an inert target in the case of a homogeneous cytoskeleton versus the transition rates $k_{m\to w}$ and $k_{w\to m}$ of the searcher for $R_{\text{d}} = 0.1$. The upper panel displays the MFPT for detection by encounter, whereas detection depends on the waiting state in the lower panel. We find that $k^{\text{opt}}_{w\to m} = \infty$ is optimal for both detection modes and all values of the detection radius R_{d}. Moreover, $k^{\text{opt}}_{m\to w} = 0$ is universally optimal for detection by encounter, whereas $k^{\text{opt}}_{m\to w}$ depends on R_{d} when detection is only possible in the waiting state, as demonstrated by Fig. 5 *e*. To investigate the impact of inhomogeneous cytoskeleton organizations, we evaluate the MFPT to an immobile target in Fig. 5 *f* as a function of p_{antero} and δ for both detection modes, in which the optimal transition rates for the homogeneous counterparts are applied. For all widths δ of the actin cortex, an optimal strategy to detect an immobile target within the cell is

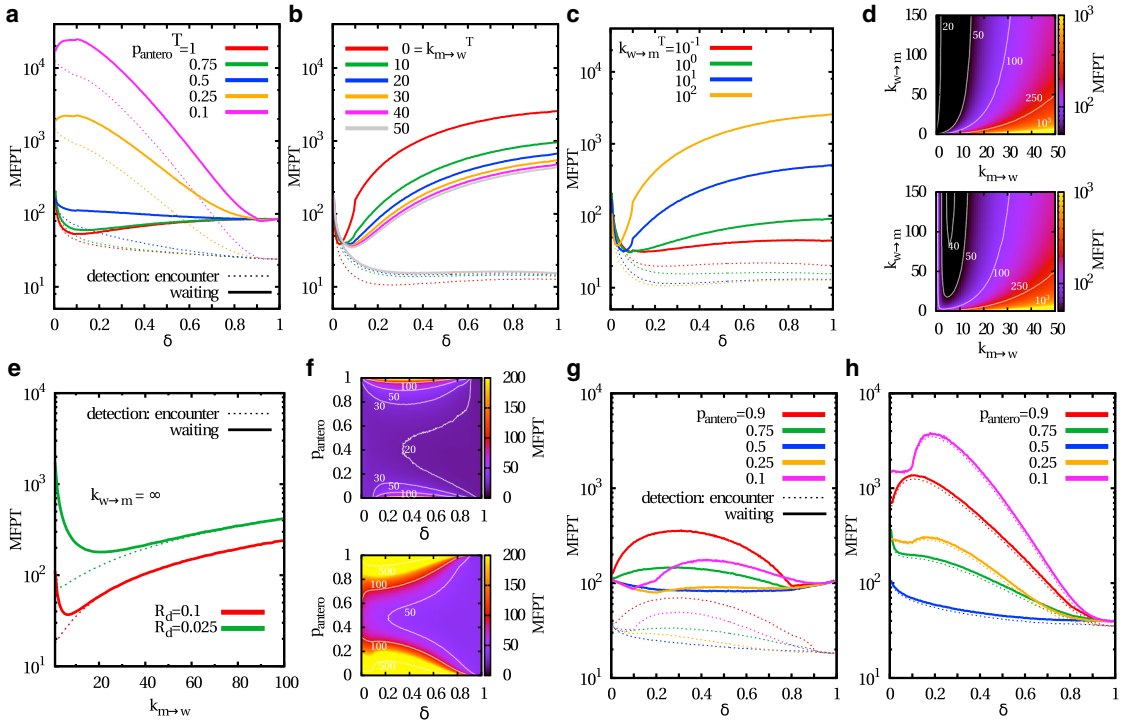

FIGURE 5 Reaction problem for nonidentical particles. (*a*) Shown here is the MFPT versus δ for nonidentical values of p_{antero}. Although $p^{\text{S}}_{\text{antero}} = 1$ is fixed for the searcher, $p^{\text{T}}_{\text{antero}}$ is varied for the target particle. Apart from that, the particles are identical, i.e., $k_{m\to w} = 10$ and $k_{w\to m} = 100$. Both detection modes are considered for $R_{\text{d}} = 0.1$. (*b*) Shown here is the MFPT as a function of δ for nonidentical transition rates $k_{m\to w}$. The rate $k^{\text{T}}_{m\to w}$ is varied for the target, whereas that of the searcher is fixed to $k^{\text{S}}_{m\to w} = 0$. Other parameters are identical, i.e., $k_{w\to m} = 100$, $p_{\text{antero}} = 1$, and $R_{\text{d}} = 0.1$. (*c*) Shown here is the MFPT versus δ for nonidentical transition rates $k_{w\to m}$. The rate $k^{\text{T}}_{w\to m}$ of the target particle is varied, whereas that of the searcher is given by $k^{\text{S}}_{w\to m} = 100$; otherwise $k_{m\to w} = 0$, $p_{\text{antero}} = 1$, and $R_{\text{d}} = 0.1$. (*d*) Shown here is the reaction problem for an immobile, uniformly distributed target particle and a homogeneous cytoskeleton as a function of the transition rates $k_{m\to w}$ and $k_{w\to m}$ of the searcher for $R_{\text{d}} = 0.1$. The upper panel shows the results when detection takes place by encounter, whereas for the lower one detection depends on the waiting state. (*e*) Shown here is the MFPT versus the transition rate $k_{m\to w}$ for an immobilized target and homogeneous cytoskeleton, where $k_{w\to m} = \infty$ and $R_{\text{d}} \in \{0.025; 0.1\}$. Both detection modes are applied. (*f*) Shown here is the MFPT versus δ and p_{antero} for an immobile target and $R_{\text{d}} = 0.1$. The optimal transition rates for the homogeneous pendant are applied for both detection modes, i.e., (*upper panel*) $k^{\text{opt}}_{m\to w} = 0$ and $k^{\text{opt}}_{w\to m} = \infty$ for detection by encounter and (*lower panel*) $k^{\text{opt}}_{m\to w} = 7$ and $k^{\text{opt}}_{w\to m} = \infty$ when detection is only possible in the waiting state. (*g*) Shown here is the MFPT as a function of δ for an immobile target and various p_{antero}. Both detection modes are considered for $R_{\text{d}} = 0.1$, $k_{m\to w} = 1$, and $k_{w\to m} = \infty$. (*h*) Shown here is the same as in (*g*), but for $k_{m\to w} = 10$. To see this figure in color, go online.

defined by $p_{\text{antero}} = 0.5$. In general, a homogeneous, random cytoskeletal network ($\delta = 1$, independent of p_{antero}) is most efficient. This conclusion is very robust against changes in the transition rates $k_{m\to w}$ and $k_{w\to m}$ and holds for both detection modes, as indicated by Fig. 5, *g* and *h*. Although the reaction problem for two identically motile particles can be efficiently solved by restricting motility space (either by $p_{\text{antero}} = 0$ and $\delta = 0$ or by $p_{\text{antero}} = 1$ and a thin cortex δ; see Fig. 4), it is best to explore the cell on a homogeneous network ($\delta = 1$ or at least $p_{\text{antero}} = 0.5$) in the case of randomly distributed immotile targets.

Reaction-escape problem

Next, we study the efficiency of inhomogeneous search strategies for the combination of reaction and escape problem. Cargo first has to bind to a reaction partner before the product can be delivered to a specific area on the cell boundary. All particles obey the same motility scheme. Fig. 1 *c* shows a sketch of the reaction-escape problem. The searcher and the target particle react and form a product particle once they get closer than a distance R_{d}, either regardless of their motility state or only possible in the waiting state. Then, the product particle performs the escape problem, as the exit area is only absorbing for the product. The total MFPT of the reaction-escape problem is composed of the $\text{MFPT}_{\text{react}}$ for the reaction problem and the $\text{MFPT}_{\text{escape}}$ for the following escape problem of the product particle to the exit zone on the plasma membrane, i.e., $\text{MFPT} = \text{MFPT}_{\text{react}} + \text{MFPT}_{\text{escape}}$.

Fig. 6, *a* and *b* present the MFPT for the reaction-escape problem in the case of a homogeneous cytoskeleton ($\delta = 1$) as a function of the rates $k_{m\to w}$ and $k_{w\to m}$ for $R_{\text{d}} = 0.1$ and $\alpha_{\text{exit}} = 0.1$. As expected, when reaction does not depend on the motility state of the particles, the MFPT is minimal for $k^{\text{opt}}_{m\to w} = 0$ and $k^{\text{opt}}_{w\to m} = \infty$, since the MFPT of the homogeneous escape problem and that of the homogeneous reaction problem is optimal for the same rates, as

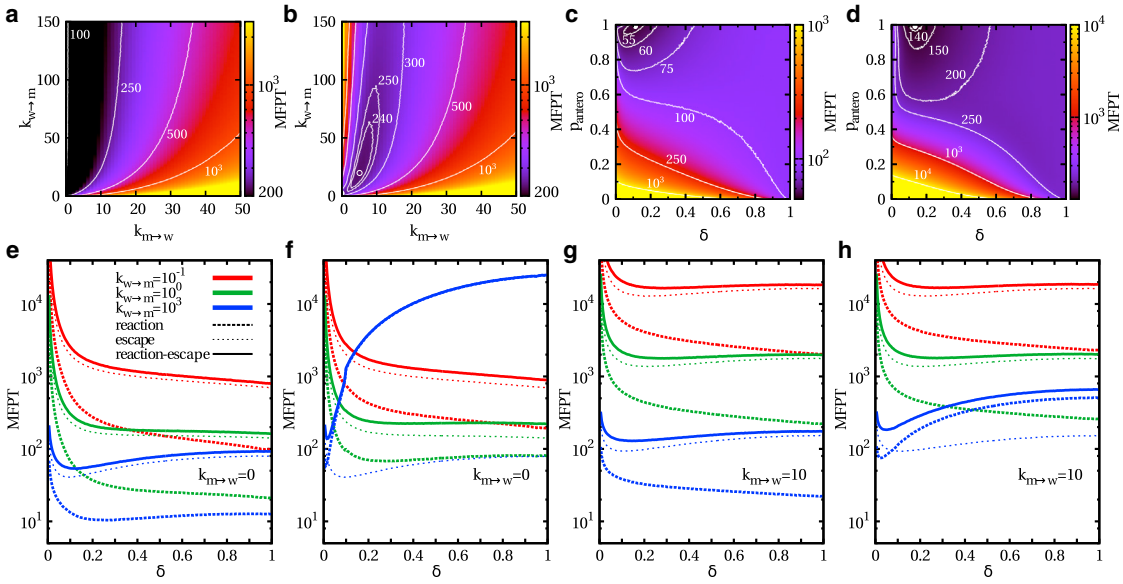

FIGURE 6 Reaction-escape problem for homogeneous and inhomogeneous spatial organizations of the cytoskeleton. (*a*) Shown here is the MFPT versus the transition rates $k_{m\to w}$ and $k_{w\to m}$ for a homogeneous cytoskeleton organization with reaction radius $R_\mathrm{d} = 0.1$ and exit size $\alpha_\mathrm{exit} = 0.1$, in which reaction happens by encounter regardless of the motility state. (*b*) Shown here is the same as in (*a*), but reaction is only possible in the waiting state. (*c*) Shown here is the MFPT as a function of the actin cortex width δ and the probability for anterograde transport p_antero for $k^\mathrm{opt}_{m\to w} = 0$, $k^\mathrm{opt}_{w\to m} = \infty$, $R_\mathrm{d} = 0.1$, and $\alpha_\mathrm{exit} = 0.1$. Reaction happens by pure encounter. (*d*) Shown here is the same as in (*c*), but for $k^\mathrm{opt}_{m\to w} = 5$ and $k^\mathrm{opt}_{w\to m} = 22$. Reaction is only possible when both particles are in the waiting state. (*e*) Shown here is the MFPT against the width of the actin cortex δ for $k_{m\to w} = 0$ and diverse values of $k_{w\to m}$, where $p_\mathrm{antero} = 1$, $R_\mathrm{d} = 0.1$, and $\alpha_\mathrm{exit} = 0.1$. Reaction happens by simple encounter. (*f*) Shown here is the same as in (*e*), but reaction depends on the waiting state. (*g*) Shown here is the same as in (*a*), but for $k_{m\to w} = 10$. (*h*) Shown here is the same as in (*f*), but for $k_{m\to w} = 10$. To see this figure in color, go online.

displayed in Figs. 2 *c* and 3 *a*. However, when reaction is only possible in the waiting state, the MFPT features two minima as a result of the interplay between $k_{m\to w} = 0$ and $k_{w\to m} = \infty$ being optimal for the escape and $k_{m\to w} = 13$ and $k_{w\to m} = 34$ being optimal for the reaction problem. Although the global minimum at $k_{m\to w} = 0$ and $k_{w\to m} = 1$ is deficient, the local minimum at $k^\mathrm{opt}_{m\to w} = 5$ and $k^\mathrm{opt}_{w\to m} = 22$, with an absolute value only 5% higher than the one of the global minimum, is very pronounced and robust against alterations of the rates.

To explore the influence of the spatial inhomogeneity of the cytoskeleton, we measure the MFPT for the reaction-escape problem as a function of the cortex width δ and the probability for anterograde transport p_antero in Fig. 6, *c* and *d* for both reaction modes, for which we used the optimal transition rates $k^\mathrm{opt}_{m\to w}$ and $k^\mathrm{opt}_{w\to m}$ of the homogeneous case. Even though $p_\mathrm{antero} = 0$ is advantageous for the pure reaction problem, as found in Fig. 4, a low probability of radially outward transport is highly inferior for the reaction-escape problem, as it prevents the compound particle from reaching the membrane and thus from detecting the exit zone. A superior search strategy for the reaction-escape problem is defined by a high probability p_antero and a thin actin cortex δ. The gain in search efficiency by an inhomogeneous spatial organization of the cytoskeleton is also conserved for nonoptimal transition rates $k_{m\to w}$ and $k_{w\to m}$, as illustrated in Fig. 6, *e–h*. Consequently, adjustments of the width of the actin cortex potentially reduce the MFPT up to several orders of magnitude.

Toward a more realistic cytoskeleton

So far, we have studied intracellular search strategies in 2D environments. However, a generalization of our model to three-dimensional (3D) spherical cells is straightforward. When updating the particle direction, the new velocity $\boldsymbol{v}^\star(v, \theta^\star_v, \varphi^\star_v)$ is given in a rotated coordinate system where the $z^\star$ axis is pointing in the direction of the current particle position $\boldsymbol{r}(r, \theta_r, \varphi_r)$. Although $\varphi^\star_v$ is uniformly distributed in $[0; 2\pi)$, the azimuth $\theta^\star_v \in [0; \pi]$ is drawn from the rotation angle distribution

$$f_\mathrm{3D}(\alpha_\mathrm{rot}) = \begin{cases} p_\mathrm{a.}\,\delta(\alpha_\mathrm{rot}) + (1 - p_\mathrm{a.})\delta(\alpha_\mathrm{rot} - \pi), & \text{for } 0 < r < R_\mathrm{m} - \delta, \\ 1/\pi, & \text{for } R_\mathrm{m} - \delta < r < R_\mathrm{m}, \end{cases} \tag{4}$$

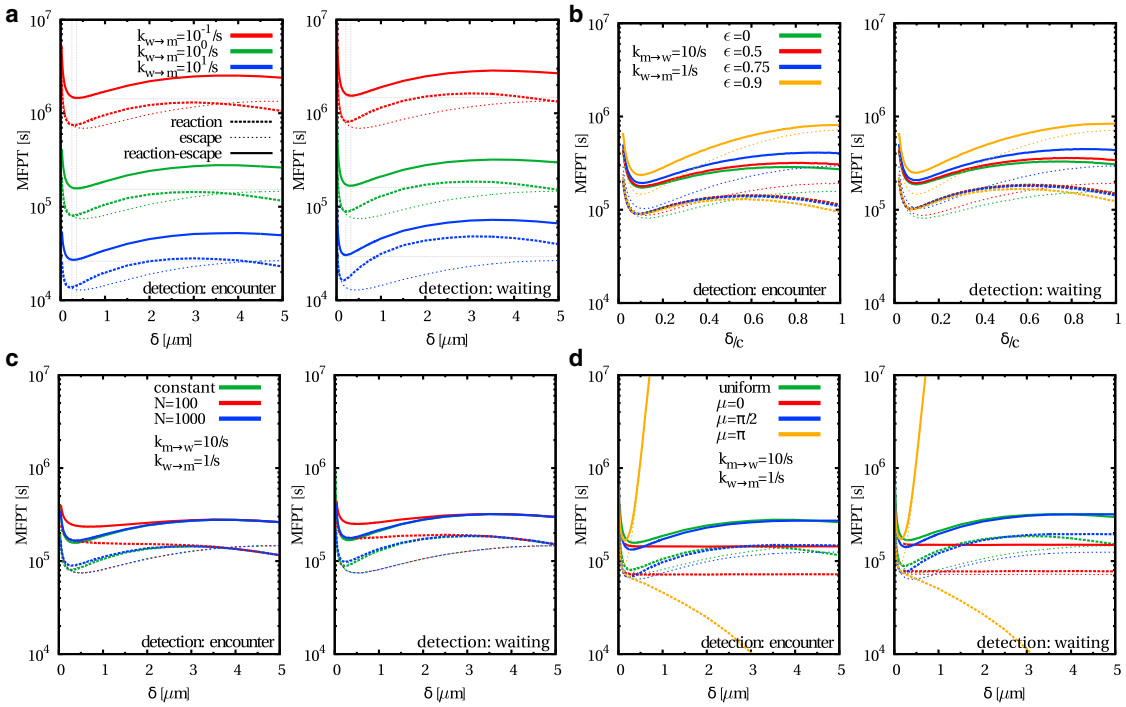

FIGURE 7 Steps toward a more realistic cytoskeleton. Given here are the MFPT of the escape, the reaction, and the reaction-escape problem as a function of the actin cortex width δ for a three-dimensional cell of volume $V = 4\pi(5\ \mu\text{m})^3/3$ with $\alpha_{\text{exit}} = 0.2$, $R_{\text{d}} = 0.1\ \mu$m, $v = 1\ \mu\text{m}/s$, and $p_{\text{antero}} = 1$. For biologically reasonable transition rates $k_{m\to w} = 10/\text{s}$ and $k_{w\to m} \in \{10^{-1}/\text{s}; 10^{0}/\text{s}; 10^{1}/\text{s}\}$, the reaction mode (*left-hand side* for reaction by pure encounter and *right-hand side* for reaction that is only possible in the waiting state) has no major impact on the search efficiency. (*a*) The optimal width of the actin cortex is approximately $\delta^{\text{opt}} = 0.3\ \mu$m in the case of a uniform distribution of actin filaments (according to Eq. 4) in spherical cells. (*b*) Shown here is the influence of cell shape on the search efficiency of transport tasks in spheroidal cells with semiaxes $c > a$ and various eccentricities ϵ. (*c*) Shown here is the MFPT for space-dependent transition rates $\tilde{k}_{w\to m}(r)$ and a total mean number of microtubules in a spherical cell of $N_{\text{MT}} \in \{10^2; 10^3\}$ in comparison to constant waiting times. (*d*) Shown here is the impact of Gaussian-distributed actin orientations with mean $\mu \in \{0; \pi/2; \pi\}$ and standard deviation $\sigma = 1$ on the MFPT in comparison to a uniformly random actin network for spherical cells. To see this figure in color, go online.

which is the 3D complement of Eq. 3. In Fig. 7, *a*, *c*, and *d*, we assume a 3D spherical cell of radius $R_{\text{m}} = 5\ \mu$m, which is consistent with the dimension of T cells. Since the diameter of an immunological synapse is reported to be of the order of microns (37,39,40,53), we choose $\alpha_{\text{exit}} = 0.2$, which results in an exit zone of size $0.2 \times 5\ \mu\text{m} = 1\ \mu$m. We further take into account the typical size of vesicles by $R_{\text{d}} = 0.1\ \mu$m (53) and the conventional motor speed by $v = 1\ \mu\text{m}/\text{s}$ (6). Since cargo typically detaches at network intersections (12), a transition rate of $k_{m\to w} = v/\ell = 10/\text{s}$ results in a biologically reasonable mesh size of $\ell = 100$ nm (35,36). We consider $k_{w\to m} \in \{10^{-1}/\text{s}; 10^{0}/\text{s}; 10^{1}/\text{s}\}$, because the mean waiting time of cargo at network intersections is reported to be of the order of seconds (12,18,58), and choose $p_{\text{antero}} = 1$, which is optimal for the reaction-escape problem as found in Fig. 6 and reflects a low activity level of dynein motors.

Under these circumstances, Fig. 7 *a* reveals an optimal width of the actin cortex of approximately $\delta^{\text{opt}} = 0.3\ \mu$m. This is in good agreement with the typical width of an actin cortex (35,36,59). Remarkably, for biologically reasonable parameters, the reaction mode has no significant effect on the search efficiency, as already expected by Fig. 3 *e* (here, the dimensionless transition rate is $k_{m\to w} \mapsto R_{\text{m}} k_{m\to w}/v = 50$). Moreover, the divergence of the MFPT in the limit of $\delta \to 0$ outlines the role of the actin cortex between functional gateway (optimized δ) and transport barrier ($\delta \to 0$) (60).

Still, Eq. 4 reflects a simplified view of the real cytoskeleton. Next, we take three steps toward a more realistic cytoskeletal organization.

Until now we investigated nonpolarized spherical cells. However, most cells show some sort of polarization (6). To check for the influence of polarization on the search efficiency of intracellular transport, we investigate ellipsoidal cells. The cell shape is modeled by a prolate spheroid with z as the symmetry axis and semiaxes c, a ($c > a$). In Fig. 7 *b*, we fix the volume of the spheroid $V = 4\pi(5\ \mu\text{m})^3/3$ to exclude volume effects and vary the eccentricity $\epsilon = \sqrt{1 - a^2/c^2} \in [0; 1[$, where $\epsilon = 0$ corresponds to a spherical cell. For the narrow escape problem, the exit zone is located at the north pole of the spheroid. Note that α_{exit} is adapted to the eccentricity ϵ to guarantee a fixed target size of $1\ \mu$m. Under biologically reasonable conditions, Fig. 7 *b* indicates

that the gain in search efficiency by a thin actin cortex is conserved for ellipsoidal cells.

Next, we consider that the concentration of microtubules is not constant but depends on the radial position r within the cell. Although the microtubule network is denser close to the MTOC, it gets more and more dilute in the cell periphery. The probability of finding a microtubule decreases with increasing r and can be estimated by $\rho_{2D}(r) = N_{MT} d_{MT}/(2\pi r)$ in 2D and $\rho_{3D}(r) = N_{MT} d_{MT}^2/(16 r^2)$ in 3D, where $N_{MT} = 10^2 - 10^3$ specifies the mean number of microtubules in the cell (61,62) and $d_{MT} = 25$nm is the diameter of a single microtubule (6). This can be considered in our model by introducing position-dependent transition rates $\tilde{k}_{w\to m}(r) = \rho(r) \times k_{w\to m}$ in the cell interior. Consequently, the greater the distance from the MTOC—and thus the lower the microtubule density—the longer the particle remains in the waiting state. Fig. 7 *c* shows the MFPT for space-dependent transition rates $\tilde{k}_{w\to m}(r)$ in comparison to the results for constant transition rate $k_{w\to m}$. As expected, the impact of the variable microtubule density on the search efficiency vanishes with increasing width of the actin cortex δ, since in the periphery the rate $k_{w\to m}$ is constant. Furthermore, the effect is stronger for low values of N_{MT} because of the resulting greater mean waiting time per waiting period. Overall, the gain in efficiency by a thin actin cortex is conserved for the reaction-escape problem.

Even though the orientation of actin filaments in the cortex typically is random, the exact distribution of actin polarities is elusive. There are several mechanisms that influence the directionality of actin networks. For instance, actin filaments align to microtubules (63) or form branches at distinct angles by means of the protein complex Arp2/3 (64,65). In Fig. 7 *d*, we analyze nonuniform, cutoff-Gaussian rotation angle distributions in the cell cortex as follows:

$$\tilde{f}_{3D}(\alpha_{rot}) = \begin{cases} p_{a.}\,\delta(\alpha_{rot}) + (1-p_{a.})\delta(\alpha_{rot}-\pi), & \text{for } 0 < r < R_m - \delta, \\ \dfrac{\mathcal{N}}{\sqrt{2\pi}} e^{-\frac{1}{2}(\alpha_{rot}-\mu)^2}, & \text{for } R_m - \delta < r < R_m, \end{cases} \tag{5}$$

with mean $\mu > 0$ and normalization $\mathcal{N}$ so that $\alpha_{rot} \in [0;\pi]$. A mean value $\mu \in [0;\pi/2)$ ($\mu \in (\pi/2;\pi]$) leads to actin filaments which are directed radially outwards (inwards), whereas $\mu = \pi/2$ corresponds to a predominantly lateral orientation. Fig. 7 *d* displays the MFPT as a function of the cortex width δ for diverse polarities of the actin cortex defined by the mean values $\mu \in \{0;\pi/2;\pi\}$. The behavior of the MFPT for lateral actin orientations ($\mu = \pi/2$) is similar to that of uniformly random actin networks because of the equal probability for outward- and inward-directed cargo transport. An inhomogeneous cytoskeletal structure with a thin actin cortex generally supports the search efficiency. On the contrary, for outward-pointing actin filaments ($\mu < \pi/2$), the particle is predominantly moving in close proximity of the cell boundary because of the actin network polarity. For that reason, the cortex width δ largely does not influence the MFPT and the homogeneous limit $\delta = 1$ is most efficient. Inward-directed actin polarities ($\mu > \pi/2$) drive the cargo toward the cell center. Although this is advantageous for the pure reaction problem (the effect is comparable to $p_{antero} = 0$ in Fig. 4), it is highly disadvantageous for the escape and consequently also for the reaction-escape problem. There, an efficient search strategy strongly depends on the formation of a thin actin cortex which forces the particle closer to the membrane, as evident from the pronounced minimum of the MFPT. In general, a larger standard deviation of the Gaussian in Eq. 5 randomizes the actin network. Consequently, the behavior of the MFPT converges to the uniform case, and an inhomogeneous cytoskeleton generally improves the search efficiency again (see also (54)).

DISCUSSION

We analyzed the importance of the spatial organization of the cytoskeleton of living cells for targeted intracellular transport, which occurs when cargo particles have to find reaction partners or specific target areas inside a cell. Motor-assisted transport along cytoskeletal filaments is known to enhance reaction kinetics in cells that are homogeneously filled with random filaments (29). However, such a condition is only fulfilled in a thin actin cortex underneath the plasma membrane, since the interior of the cell allows merely radial transport along microtubules.

Remarkably, we find that the confinement of randomly oriented cytoskeletal filaments to a thin actin cortex is not a handicap for the cell but can substantially increase the efficiency of diverse transport tasks. We obtain this result by formulation of a random velocity model with intermittent arrest states that takes into account the spatially inhomogeneous structure of the cytoskeleton. Our model allows the systematic study of the impact of the cytoskeleton organization, the motor behavior, and the target detection mode on the search efficiency of diverse transport tasks. Here, we analyze three paradigmatic intracellular search problems: the narrow escape problem, the reaction problem, and the reaction-escape problem.

TABLE 1 Recapitulation of the Optimal Search Strategies for Narrow Escapes Defined by $\alpha_{exit} = 0.1$ and Reaction Partners of Size $R_d = 0.1$

	Homogeneous Cytoskeleton		Inhomogeneous Cytoskeleton	
	$k^{opt}_{m\to w}$	$k^{opt}_{w\to m}$	p^{opt}_{antero}	δ^{opt}
Narrow escape	0	∞	1	$\in\ ]0;1[$
Reaction of Identical Particles				
Detection: encounter	0	∞	0	0
Detection: waiting	$\sim$13	$\sim$34	0	0
Reaction with Immotile Target				
Detection: encounter	0	∞	0.5	1
Detection: waiting	$\sim$7	∞	0.5	1
Reaction-Escape of Identical Particles				
Detection: encounter	0	∞	1	$\in\ ]0;1[$
Detection: waiting	$\sim$5	$\sim$22	1	$\in\ ]0;1[$

The optimal transition rates $k^{opt}_{m\to w}$ and $k^{opt}_{w\to m}$ of a homogeneous cytoskeleton structure are applied for the inhomogeneous case.

We find that the best strategy for the escape problem is to transport the cargo toward the periphery by a high probability for anterograde transport and keep it in close proximity to the membrane by providing a thin actin cortex. In the case of the reaction problem, efficient detection is based on bringing the reaction partners with identical motility patterns close together either at the center of the cell ($p_{antero} = 0$ and $\delta = 0$) or in a thin cortex ($p_{antero} = 1$ and δ^{opt}). However, this strategy fails for nonidentical particles with different motor activity levels defined by p_{antero}. In that case, a homogeneous, random cytoskeleton ($\delta = 1$) is advantageous. Although for the reaction problem, $p_{antero} = 0$ is most efficient, it is highly deficient for the escape problem. Hence, both strategies have to be combined effectively for the reaction-escape problem. In the case that the motility pattern of the product particle is not different from that of searcher and target, a high probability for anterograde transport and establishing a thin actin cortex is favorable. Table 1 recapitulates the best search strategies for the three transport tasks under investigation.

Our results indicate that cells with a centrosome are able to realize efficient intracellular search strategies by intermittent transport on a cytoskeleton with specific spatial structure (see also (49,50) for similar findings in a model with intermittent diffusion). In comparison to the homogeneous pendant, an inhomogeneous cytoskeleton organization that displays only a thin actin cortex generally leads to a considerable gain in search efficiency for diverse intracellular transport tasks.

AUTHOR CONTRIBUTIONS

H.R. designed the research. A.E.H. performed calculations, prepared figures, and analyzed the data. H.R. and A.E.H. wrote the manuscript.

ACKNOWLEDGMENTS

The authors wish to thank Gleb Oshanin for helpful discussions.

This work was financially supported by the German Research Foundation (DFG) within the Collaborative Research Center SFB 1027.

REFERENCES

1. Nédélec, F. J., T. Surrey, …, S. Leibler. 1997. Self-organization of microtubules and motors. *Nature.* 389:305–308.
2. Thoumine, O., and A. Ott. 1997. Time scale dependent viscoelastic and contractile regimes in fibroblasts probed by microplate manipulation. *J. Cell Sci.* 110:2109–2116.
3. Kruse, K., J. F. Joanny, …, K. Sekimoto. 2004. Asters, vortices, and rotating spirals in active gels of polar filaments. *Phys. Rev. Lett.* 92:078101.
4. Storm, C., J. J. Pastore, …, P. A. Janmey. 2005. Nonlinear elasticity in biological gels. *Nature.* 435:191–194.
5. Mizuno, D., C. Tardin, …, F. C. Mackintosh. 2007. Nonequilibrium mechanics of active cytoskeletal networks. *Science.* 315:370–373.
6. Alberts, B., A. Johnson, …, P. Walter. 2014. Molecular Biology of the Cell, Sixth Edition. Garland Science, New York.
7. Sheetz, M. P., and J. A. Spudich. 1983. Movement of myosin-coated fluorescent beads on actin cables in vitro. *Nature.* 303:31–35.
8. Howard, J., A. J. Hudspeth, and R. D. Vale. 1989. Movement of microtubules by single kinesin molecules. *Nature.* 342:154–158.
9. Appert-Rolland, C., M. Ebbinghaus, and L. Santen. 2015. Intracellular transport driven by cytoskeletal motors: general mechanisms and defects. *Phys. Rep.* 593:1–59.
10. Schliwa, M., and G. Woehlke. 2003. Molecular motors. *Nature.* 422:759–765.
11. Vale, R. D., and R. A. Milligan. 2000. The way things move: looking under the hood of molecular motor proteins. *Science.* 288:88–95.
12. Bálint, Š., I. Verdeny Vilanova, …, M. Lakadamyali. 2013. Correlative live-cell and superresolution microscopy reveals cargo transport dynamics at microtubule intersections. *Proc. Natl. Acad. Sci. USA.* 110:3375–3380.
13. Hancock, W. O. 2014. Bidirectional cargo transport: moving beyond tug of war. *Nat. Rev. Mol. Cell Biol.* 15:615–628.
14. Vershinin, M., B. C. Carter, …, S. P. Gross. 2007. Multiple-motor based transport and its regulation by Tau. *Proc. Natl. Acad. Sci. USA.* 104:87–92.
15. Welte, M. A. 2004. Bidirectional transport along microtubules. *Curr. Biol.* 14:R525–R537.
16. Gross, S. P., M. Vershinin, and G. T. Shubeita. 2007. Cargo transport: two motors are sometimes better than one. *Curr. Biol.* 17:R478–R486.
17. Mallik, R., and S. P. Gross. 2004. Molecular motors: strategies to get along. *Curr. Biol.* 14:R971–R982.
18. Slepchenko, B. M., I. Semenova, …, V. Rodionov. 2007. Switching of membrane organelles between cytoskeletal transport systems is determined by regulation of the microtubule-based transport. *J. Cell Biol.* 179:635–641.
19. Kural, C., A. S. Serpinskaya, …, P. R. Selvin. 2007. Tracking melanosomes inside a cell to study molecular motors and their interaction. *Proc. Natl. Acad. Sci. USA.* 104:5378–5382.
20. Rodionov, V., J. Yi, …, S. P. Gross. 2003. Switching between microtubule- and actin-based transport systems in melanophores is controlled by cAMP levels. *Curr. Biol.* 13:1837–1847.
21. Bressloff, P. C., and J. M. Newby. 2013. Stochastic models of intracellular transport. *Rev. Mod. Phys.* 85:135–196.
22. Ali, M. Y., E. B. Krementsova, …, D. M. Warshaw. 2007. Myosin Va maneuvers through actin intersections and diffuses along microtubules. *Proc. Natl. Acad. Sci. USA.* 104:4332–4336.

23. Ross, J. L., M. Y. Ali, and D. M. Warshaw. 2008. Cargo transport: molecular motors navigate a complex cytoskeleton. *Curr. Opin. Cell Biol.* 20:41–47.
24. Ross, J. L., H. Shuman, …, Y. E. Goldman. 2008. Kinesin and dynein-dynactin at intersecting microtubules: motor density affects dynein function. *Biophys. J.* 94:3115–3125.
25. Weiss, M., M. Elsner, …, T. Nilsson. 2004. Anomalous subdiffusion is a measure for cytoplasmic crowding in living cells. *Biophys. J.* 87:3518–3524.
26. Yu, I., T. Mori, …, M. Feig. 2016. Biomolecular interactions modulate macromolecular structure and dynamics in atomistic model of a bacterial cytoplasm. *eLife.* 5:e19274.
27. Hafner, A. E., L. Santen, …, M. R. Shaebani. 2016. Run-and-pause dynamics of cytoskeletal motor proteins. *Sci. Rep.* 6:37162.
28. Bénichou, O., C. Loverdo, …, R. Voituriez. 2011. Intermittent search strategies. *Rev. Mod. Phys.* 83:81–129.
29. Loverdo, C., O. Bénichou, …, R. Voituriez. 2008. Enhanced reaction kinetics in biological cells. *Nat. Phys.* 4:134–137.
30. Bénichou, O., M. Coppey, …, R. Voituriez. 2005. Optimal search strategies for hidden targets. *Phys. Rev. Lett.* 94:198101.
31. Loverdo, C., O. Bénichou, …, R. Voituriez. 2009. Robustness of optimal intermittent search strategies in one, two, and three dimensions. *Phys. Rev. E Stat. Nonlin. Soft Matter Phys.* 80:031146.
32. Bénichou, O., D. Grebenkov, …, R. Voituriez. 2010. Optimal reaction time for surface-mediated diffusion. *Phys. Rev. Lett.* 105:150606.
33. Calandre, T., O. Bénichou, and R. Voituriez. 2014. Accelerating search kinetics by following boundaries. *Phys. Rev. Lett.* 112:230601.
34. Ando, D., N. Korabel, …, A. Gopinathan. 2015. Cytoskeletal network morphology regulates intracellular transport dynamics. *Biophys. J.* 109:1574–1582.
35. Eghiaian, F., A. Rigato, and S. Scheuring. 2015. Structural, mechanical, and dynamical variability of the actin cortex in living cells. *Biophys. J.* 108:1330–1340.
36. Salbreux, G., G. Charras, and E. Paluch. 2012. Actin cortex mechanics and cellular morphogenesis. *Trends Cell Biol.* 22:536–545.
37. Grakoui, A., S. K. Bromley, …, M. L. Dustin. 1999. The immunological synapse: a molecular machine controlling T cell activation. *Science.* 285:221–227.
38. Bromley, S. K., W. R. Burack, …, M. L. Dustin. 2001. The immunological synapse. *Annu. Rev. Immunol.* 19:375–396.
39. Angus, K. L., and G. M. Griffiths. 2013. Cell polarisation and the immunological synapse. *Curr. Opin. Cell Biol.* 25:85–91.
40. Ritter, A. T., K. L. Angus, and G. M. Griffiths. 2013. The role of the cytoskeleton at the immunological synapse. *Immunol. Rev.* 256:107–117.
41. Marco, E., R. Wedlich-Soldner, …, L. F. Wu. 2007. Endocytosis optimizes the dynamic localization of membrane proteins that regulate cortical polarity. *Cell.* 129:411–422.
42. Alberts, P., and T. Galli. 2003. The cell outgrowth secretory endosome (COSE): a specialized compartment involved in neuronal morphogenesis. *Biol. Cell.* 95:419–424.
43. Chada, S. R., and P. J. Hollenbeck. 2003. Mitochondrial movement and positioning in axons: the role of growth factor signaling. *J. Exp. Biol.* 206:1985–1992.
44. Andrews, N. W., P. E. Almeida, and M. Corrotte. 2014. Damage control: cellular mechanisms of plasma membrane repair. *Trends Cell Biol.* 24:734–742.
45. McNeil, P. L., and T. Kirchhausen. 2005. An emergency response team for membrane repair. *Nat. Rev. Mol. Cell Biol.* 6:499–505.
46. Schuss, Z., A. Singer, and D. Holcman. 2007. The narrow escape problem for diffusion in cellular microdomains. *Proc. Natl. Acad. Sci. USA.* 104:16098–16103.
47. Schuss, Z. 2012. The narrow escape problem - a short review of recent results. *J. Sci. Comput.* 53:194–210.
48. Granger, E., G. McNee, …, P. Woodman. 2014. The role of the cytoskeleton and molecular motors in endosomal dynamics. *Semin. Cell Dev. Biol.* 31:20–29.
49. Schwarz, K., Y. Schröder, …, H. Rieger. 2016. Optimality of spatially inhomogeneous search strategies. *Phys. Rev. Lett.* 117:068101.
50. Schwarz, K., Y. Schröder, and H. Rieger. 2016. Numerical analysis of homogeneous and inhomogeneous intermittent search strategies. *Phys. Rev. E.* 94:042133.
51. Huet, S., E. Karatekin, …, J.-P. Henry. 2006. Analysis of transient behavior in complex trajectories: application to secretory vesicle dynamics. *Biophys. J.* 91:3542–3559.
52. Cebecauer, M., M. Spitaler, …, A. I. Magee. 2010. Signalling complexes and clusters: functional advantages and methodological hurdles. *J. Cell Sci.* 123:309–320.
53. Qu, B., V. Pattu, …, M. Hoth. 2011. Docking of lytic granules at the immunological synapse in human CTL requires Vti1b-dependent pairing with CD3 endosomes. *J. Immunol.* 186:6894–6904.
54. Hafner, A. E., and H. Rieger. 2016. Spatial organization of the cytoskeleton enhances cargo delivery to specific target areas on the plasma membrane of spherical cells. *Phys. Biol.* 13:066003.
55. Arcizet, D., B. Meier, …, D. Heinrich. 2008. Temporal analysis of active and passive transport in living cells. *Phys. Rev. Lett.* 101:248103.
56. Mejía-Monasterio, C., G. Oshanin, and G. Schehr. 2011. First passages for a search by a swarm of independent random searchers. *J. Stat. Mech.* 2011:P06022.
57. Mattos, T. G., C. Mejía-Monasterio, …, G. Oshanin. 2012. First passages in bounded domains: when is the mean first passage time meaningful? *Phys. Rev. E Stat. Nonlin. Soft Matter Phys.* 86:031143.
58. Zaliapin, I., I. Semenova, …, V. Rodionov. 2005. Multiscale trend analysis of microtubule transport in melanophores. *Biophys. J.* 88:4008–4016.
59. Clark, A. G., K. Dierkes, and E. K. Paluch. 2013. Monitoring actin cortex thickness in live cells. *Biophys. J.* 105:570–580.
60. Papadopulos, A., V. M. Tomatis, …, F. A. Meunier. 2013. The cortical acto-Myosin network: from diffusion barrier to functional gateway in the transport of neurosecretory vesicles to the plasma membrane. *Front. Endocrinol. (Lausanne).* 4:153.
61. Cohen, W. D., and L. I. Rebhun. 1970. An estimate of the amount of microtubule protein in the isolated mitotic apparatus. *J. Cell Sci.* 6:159–176.
62. Schulze, E., and M. Kirschner. 1987. Dynamic and stable populations of microtubules in cells. *J. Cell Biol.* 104:277–288.
63. Preciado López, M., F. Huber, …, M. Dogterom. 2014. Actin-microtubule coordination at growing microtubule ends. *Nat. Commun.* 5:4778.
64. Mullins, R. D., J. A. Heuser, and T. D. Pollard. 1998. The interaction of Arp2/3 complex with actin: nucleation, high affinity pointed end capping, and formation of branching networks of filaments. *Proc. Natl. Acad. Sci. USA.* 95:6181–6186.
65. Risca, V. I., E. B. Wang, …, D. A. Fletcher. 2012. Actin filament curvature biases branching direction. *Proc. Natl. Acad. Sci. USA.* 109:2913–2918.